ChemPubSoc Europe

DOI: 10.1002/chem.201604286

CHEMISTRY
A European Journal
Communication

Solid Solutions |*Hot Paper*|

First-Principles Calculation, Synthesis, and Catalytic Properties of Rh-Cu Alloy Nanoparticles

Tokutaro Komatsu,*[a, b] Hirokazu Kobayashi,[a, c] Kohei Kusada,[a] Yoshiki Kubota,[d] Masaki Takata,[e, f] Tomokazu Yamamoto,[g] Syo Matsumura,[g] Katsutoshi Sato,[h, i] Katsutoshi Nagaoka,[h, i] and Hiroshi Kitagawa*[a, j, k]

Abstract: The first synthesis of pure $Rh_{1-x}Cu_x$ solid-solution nanoparticles is reported. In contrast to the bulk state, the solid-solution phase was stable up to 750 °C. Based on facile density-functional calculations, we made a prediction that the catalytic activity of $Rh_{1-x}Cu_x$ can be maintained even with 50 at% replacement of Rh with Cu. The prediction was confirmed for the catalytic activities on CO and NO_x conversions.

The design of intermetallic materials had long been limited by the immiscibility of the component metals. The advent of non-equilibrium synthetic methods has opened up the fertile field of alloy nanoparticles (NPs) by providing an easy method for production of alloy NPs on a large scale.[1] The explosion of the variety of possible alloy NPs poses another kind of difficulty in that it is unrealistic to experimentally examine every combination of metals. We have been using density-functional theory (DFT) calculations as the primary screening tool for possible candidates, by estimating target properties and relative stability of the alloy phase. Herein, we report the electronic-structure calculations, synthesis, and activities as three-way catalysts (TWCs) of NPs of Rh-Cu solid solutions. In agreement with the DFT calculation, the catalytic activities for the CO and nitrogen oxides (NO_x) conversion reactions were maintained even with the 50 at% replacement of Rh with Cu.

The Rh-Cu alloy has been extensively investigated,[2] either as surface alloys on substrates[3] or as in situ synthesised particles supported on oxides.[4] However, because of their intrinsic immiscibility at temperatures below 1100 °C[5,6] and the susceptibility of Cu for oxidation, the synthesis and isolation of Rh-Cu NPs pose a serious challenge. As a result, there have been few reports on pure $Rh_{1-x}Cu_x$ NPs to date.

Catalysts for NO_x reduction are one of crucial materials for the protection of the environment. Nitrogen oxides cause serious atmospheric pollution, resulting in acid rain, ozone depletion, and respiratory disorders. Thus, TWCs are widely used to reduce the emissions of this noxious pollutant.[7,8] One of the major sources of NO_x emissions is automobiles, where the TWC is used to convert the NO_x, CO and hydrocarbons (HCs) in the exhaust into CO_2 and N_2.[9] Rhodium has been utilised as an indispensable component in the TWC.[8] As Rh is a rare and precious element, much effort has been dedicated to reducing its usage in the TWC and/or enhancing the catalytic activity. On the other hand, copper is one of the candidate diluting elements for a TWC because of its abundance and catalytic activity for CO[10] and HC[11] oxidation.

It is well-known that the catalytic activity of a material strongly depends on the magnitude of the density of states at

[a] *Dr. T. Komatsu, Dr. H. Kobayashi, Dr. K. Kusada, Prof. Dr. H. Kitagawa*
Division of Chemistry, Graduate School of Science, Kyoto University
Kitashirakawa Oiwake-cho, Sakyo-ku, Kyoto 606-8502 (Japan)
E-mail: kitagawa@kuchem.kyoto-u.ac.jp

[b] *Dr. T. Komatsu*
Present address: School of Medicine, Nihon University
30-1 Oyaguchi-Kamicho, Itabashi-ku, Tokyo 173-8610 (Japan)
E-mail: komatsu.tokutaro@nihon-u.ac.jp

[c] *Dr. H. Kobayashi*
JST PRESTO, 4-1-8 Honcho, Kawaguchi, Saitama 332-0012 (Japan)

[d] *Prof. Dr. Y. Kubota*
Department of Physical Science, Graduate School of Science, Osaka Prefecture University, 1-1 Gakuen-cho, Naka-ku, Sakai, Osaka 599-8531 (Japan)

[e] *Prof. Dr. M. Takata*
RIKEN SPring-8 Center
1-1-1 Kouto, Sayo-cho, Sayo-gun, Hyogo 679-5148 (Japan)

[f] *Prof. Dr. M. Takata*
Japan Synchrotron Radiation Research Institute
1-1-1 Kouto, Sayo-cho, Sayo-gun, Hyogo 679-5198 (Japan)

[g] *T. Yamamoto, Prof. Dr. S. Matsumura*
Department of Applied Quantum Physics and Nuclear Engineering
Kyushu University, Nishi-ku, Fukuoka, 819-0395 (Japan)

[h] *Dr. K. Sato, Dr. K. Nagaoka*
Department of Applied Chemistry, Faculty of Engineering
Oita University, 700 Dannoharu, Oita 870-1192 (Japan)

[i] *Dr. K. Sato, Dr. K. Nagaoka*
Center for the Promotion of Interdisciplinary Education and Research
Unit of Elements Strategy Initiative for Catalysts & Batteries (ESICB)
Kyoto University, 1-30, Goryo Ohara, Nishikyo-ku, Kyoto 615-8503 (Japan)

[j] *Prof. Dr. H. Kitagawa*
Institute for Integrated Cell-Material Sciences (iCeMS)
Kyoto University, Yoshida, Sakyo-ku, Kyoto 606-8501 (Japan)

[k] *Prof. Dr. H. Kitagawa*
INAMORI Frontier Research Center, Kyushu University
744 Motooka, Nishi-ku, Fukuoka, 819-3095 (Japan)

Supporting information for this article can be found under: http://dx.doi.org/10.1002/chem.201604286.

the Fermi level (DOS(E_F))[12] and the position of the weighted centre of filled d band, namely, the d-band centre.[13] To obtain rough estimates of the catalytic activities and stabilities of Rh-Cu alloy NPs, we performed theoretical calculations. The band structures for $Rh_{1-x}Cu_x$ were calculated on periodic models with a 2×2×2 supercell. The calculations reproduced the relative stability of the alloy phase[6] and the *x*-dependence of the lattice constant[14] fairly well (Supporting Information, Figures S1, S2). According to the cubic symmetry, the 32 sites were classified into 6 groups of equivalent positions (Supporting Information, Table S1). Figure 1 (see the Supporting Information, Figure S3 for more details) shows the partial density of states (PDOS) and the DOS of $Rh_{1-x}Cu_x$. As shown in Figure 1, the DOS(E_F) of $Rh_{1-x}Cu_x$ is mainly composed of the PDOS(E_F) of Rh in the Rh-rich region. With increasing Cu content ($x \geq 0.75$), the contribution of the PDOS(E_F) of Cu increases, resulting in a decrease of the total DOS(E_F).

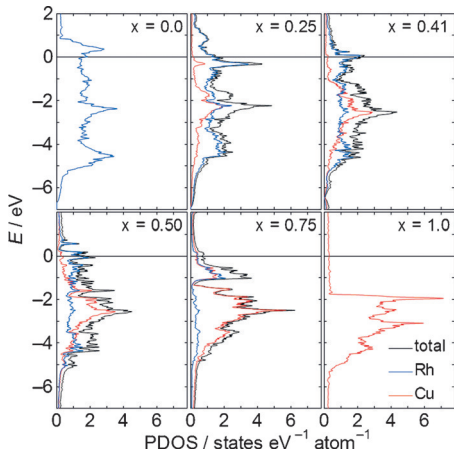

Figure 1. Partial density of states (PDOS) of $Rh_{1-x}Cu_x$.

It should be noted that in Figure 1, a narrow band was formed in the Cu-rich region, that is, $0.75 \leq x \leq 0.94$, at 0.7 eV below E_F. Therefore, the DOS(E_F) for the Cu-rich $Rh_{1-x}Cu_x$ NPs would be greatly enhanced by lowering E_F (for example, the DOS for $x = 0.81$ is shown in the Supporting Information, Figure S4). If the catalytic activity actually scales with the DOS(E_F), it is proposed that $Rh_{0.19}Cu_{0.81}$ NPs on an electron-withdrawing support would show comparable catalytic activity to that of Rh NPs. In other words, the Rh content in TWCs might be reduced by 80%. Our results suggest that the DOS of 3d–4d systems can be controlled not only by the superposition of the bands but also by the formation of new bands.

From the band structures given in the Supporting Information, Figure S3, the DOS(E_F) and d-band centre of $Rh_{1-x}Cu_x$ were calculated (Figure 2). The constraint of the site distribution allows several models for the same composition, that is, the DOS(E_F) of 4 models are plotted for $x = 0.5$. The scattering of the calculated DOS(E_F) indicates the sensitivity of the DOS to the local structures.

It should be noted that the DOS(E_F) and the position of the *d*-band centre show almost the same *x*-dependence. Since

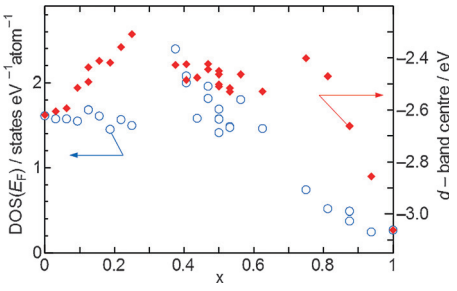

Figure 2. Density of states at Fermi level (DOS(E_F)) and d-band centre of $Rh_{1-x}Cu_x$ plotted against *x*.

both of the parameters for $x = 0.5$ are comparable to those for $x = 0.0$, we can expect similar catalytic activities of $Rh_{0.5}Cu_{0.5}$ alloy NPs as those of the pure Rh NPs.

Based on the prediction of DFT calculations, we synthesised $Rh_{1-x}Cu_x$ alloy NPs with $0 < x < 0.81$. The $Rh_{1-x}Cu_x$ alloy NPs were synthesised by a modified polyol reduction method, in which the reducing ability of ethylene glycol is enhanced by the addition of strong base. As an example, the synthetic procedure for $x = 0.50$ is described in detail below. Anhydrous rhodium(III) acetate (Mitsuwa Chemicals, 148.6 mg (0.531 mmol)) and anhydrous copper(II) chloride (Nacalai Tesque, 75.9 mg, 0.565 mmol), poly(*N*-vinyl-2-pyrrolidone) (Wako Pure Chemical Industries, 137.8 mg), and potassium *tert*-butoxide (Tokyo Chemical Industry, 412.2 mg (3.67 mmol)) were dissolved in 20 mL of anhydrous ethylene glycol (Sigma–Aldrich) to form a dark-green solution. The atomic ratio of Cu to Rh was 1.06. The solution was added dropwise to 200 mL of triethylene glycol (Tokyo Chemical Industry) at 218–221 °C with magnetic stirring. The colour of the reaction mixture immediately turned dark brown. After cooling to room temperature, the NPs were centrifuged and successively washed with acetone, ultrapure water, ethanol, and diethyl ether and subsequently dried. The atom ratio of Rh and Cu for the NPs was determined to be 0.50:0.50 using energy-dispersive X-ray spectroscopy (EDS). The atomic ratio of the metal precursors controlled the Cu content in the $Rh_{1-x}Cu_x$ alloy NPs (Supporting Information, Figure S5). Reactions without strong base or at lower temperatures inevitably resulted in phase-separated NPs of Rh and Cu, especially for large *x*. This tendency indicates that the simultaneous reduction of the Rh and Cu precursors has a key role in producing the solid-solution NPs.

The obtained $Rh_{1-x}Cu_x$ alloy NPs were characterised by the transmission electron microscopy (TEM) and powder X-ray diffraction (PXRD) measurements. TEM images (Figure 3) show that the alloy NPs were monodispersed and spherical. The mean diameters of the alloy NPs were estimated to be 1.6, 1.7, 1.9, 3.2, and 4.0 nm for $x = 0.0$, 0.17, 0.50, 0.69, and 0.81, respectively (Supporting Information, Figure S6), and the diameters slightly increased with increasing Cu content.

The PXRD patterns for $x = 0.17$–0.81 are shown in Figure 4. The Rietveld refinements of the PXRD patterns revealed that all of the $Rh_{1-x}Cu_x$ alloy NPs are single phase with a face-centred cubic structure (Figure 4; Supporting Information, Figures S7–S10). The lattice constants of the NPs showed a slight

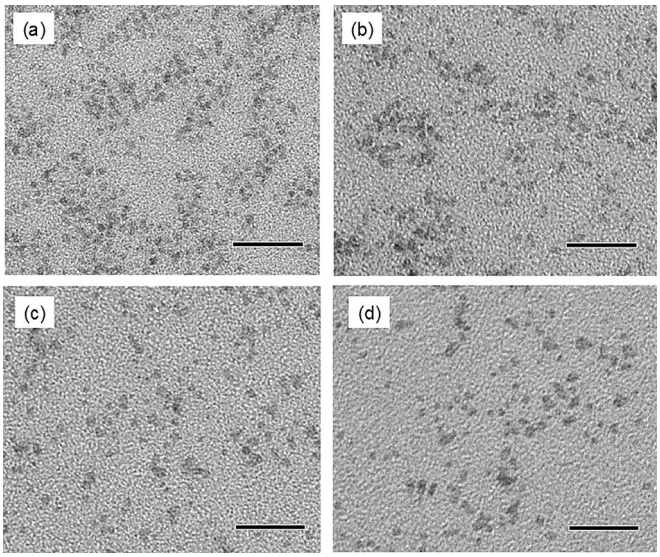

Figure 3. TEM images of $Rh_{1-x}Cu_x$ nanoparticles with x values of a) 0.17, b) 0.50, c) 0.69, and d) 0.81. Scale bars: 20 nm.

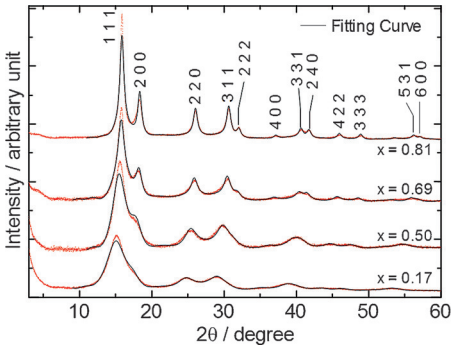

Figure 4. PXRD patterns and fitting curves of Rietveld refinement for $Rh_{1-x}Cu_x$ nanoparticles with $x = 0.17$–0.81.

deviation from Vegard's law (Supporting Information, Figure S11), similar to the case of the bulk alloys.[6,14] It should also be noted that the Cu-rich sample ($x = 0.81$) did not contain any crystalline impurities, such as Cu_2O. As Cu is easily oxidised, the synthesis of pure, Cu-rich $Rh_{1-x}Cu_x$ NPs is still challenging. In fact, a previous study reported that Rh-Cu alloy NPs with 60 at% of Cu included Cu_2O.[15] Our method provides an effective synthetic route not only for solid-solution alloy NPs of elements that are immiscible in the bulk state but also for alloys composed of an easily oxidised element.

To investigate the structure of the alloys in detail, we performed high-angle annular dark-field scanning TEM (HAADF-STEM) imaging (Figure 5a) and elemental mapping with EDS. The EDS mappings of Cu, Rh, and their superposition (Figures 5b–d) indicated that Rh and Cu were atomically mixed in the NPs without clear phase separation. In contrast, it is well-known that in the bulk Rh-Cu system, Rh and Cu are immiscible below 1100 °C.[5,6] Interestingly, the alloy structure of $Rh_{0.5}Cu_{0.5}$ was stable up to 750 °C (Supporting Information, Figure S12), which is presumably due to the nanosize effect.

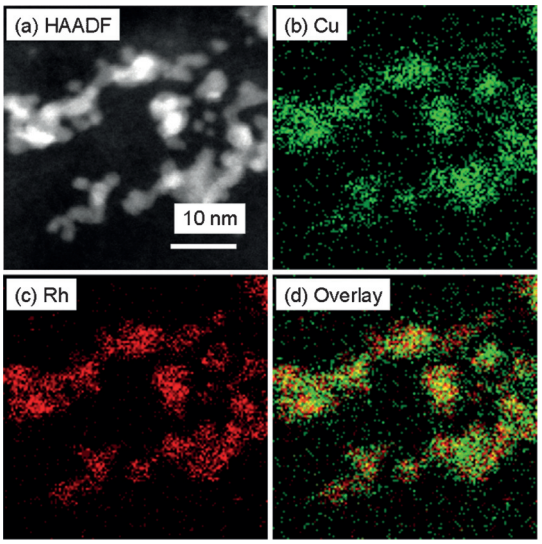

Figure 5. a) HAADF-STEM image and b)–d) STEM-EDS mappings of Cu-K (b), Rh-L (c), and overlay (d) for $Rh_{0.50}Cu_{0.50}$.

Having confirmed the solid-solution phase of the $Rh_{1-x}Cu_x$ NPs, we measured the TWC activities of the $Rh_{1-x}Cu_x$ NPs with $x = 0$, 0.50, and 0.81 (Figure 6a,b; Supporting Information, Figure S13). The CO and NO_x conversions by $Rh_{0.50}Cu_{0.50}$ and $Rh_{0.19}Cu_{0.81}$ alloy NPs increased smoothly with increasing tem-

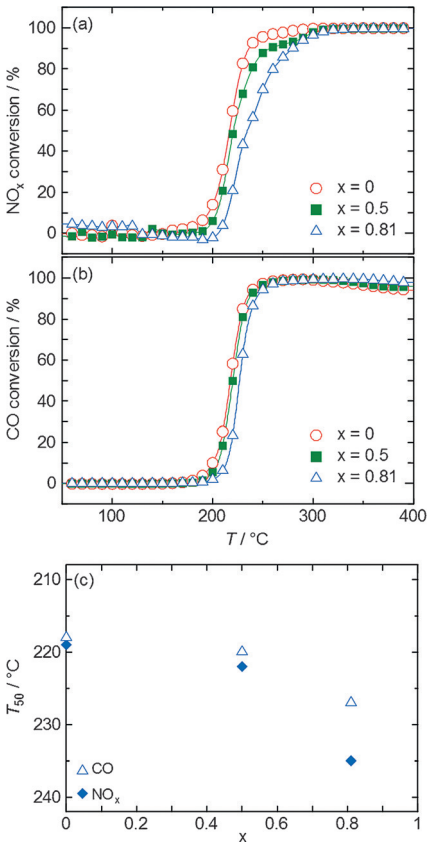

Figure 6. Temperature dependence of a) NO_x and b) CO conversion of $Rh_{1-x}Cu_x$ nanoparticles in three-way catalytic reaction and c) the catalytic activity (T_{50}) of $Rh_{1-x}Cu_x$ plotted against x.

perature, as did the conversions for the Rh NPs with a diameter of 1.6 nm. The temperatures at which 50% of CO or NO_x were converted (T_{50}) were plotted against x in Figure 6c. The T_{50} values of CO and NO_x for $Rh_{0.50}Cu_{0.50}$ NPs were 220 and 222 °C, respectively, while those for $Rh_{0.19}Cu_{0.81}$ NPs were 227 and 235 °C. Increasing the Cu content in the alloy NPs reduced the catalytic activities. It should be noted that the T_{50} values of the $Rh_{0.50}Cu_{0.50}$ NPs were almost the same as those of pure Rh NPs (218 and 219 °C for CO and NO_x, respectively). These results confirmed the predictions of DFT calculations that the activities for the CO and NO_x conversions can be maintained even when 50 at% of the rare and expensive Rh is replaced by the abundant Cu. It should also be noted that the diameter of the $Rh_{0.50}Cu_{0.50}$ NPs (1.9 nm) is slightly larger than that of the Rh NPs (1.6 nm). Assuming that the surface-atom ratio is inversely proportional to the diameter, the measured catalytic activity of the $Rh_{0.50}Cu_{0.50}$ NPs may be reduced by the large particle size. The size dependence of catalytic activities of $Rh_{1-x}Cu_x$ are currently under investigation. The persistent catalytic activities of the Rh-Cu alloy NPs also indicate that the alloy NPs form not phase-separated structure but solid-solution one, because, in the former case, the catalytic activity would decrease linearly with increasing x. On the other hand, the T_{50} values for HC conversion (Supporting Information, Figure S14) were substantially higher than those for CO and NO_x, which is probably due to a different reaction mechanism for HC conversion than for the CO and NO_x conversions.

In conclusion, we synthesised $Rh_{1-x}Cu_x$ nanoparticles, where Rh and Cu are mixed at the atomic level over a wide composition range ($x = 0.17$–0.81), for the first time. In contrast to the bulk state, the alloy phase of the nanoparticles was stable up to 750 °C. The catalytic activities for CO and NO_x conversions were maintained even with 50 at% replacement of Rh with Cu, in agreement with the calculated DOS(E_F) and d-band centre values.

Acknowledgements

This work was supported by the MEXT Project for Developing Innovation Systems (Regional Innovation Strategy Support Program "Kyoto Next-Generation Energy System Creation Strategy"). The calculations were performed on the supercomputer of ACCMS, Kyoto University and SuperComputer System, Institute for Chemical Research, Kyoto University.

Keywords: copper · density-functional calculations · heterogeneous catalysis · nanoparticles · rhodium

[1] H. Kobayashi, K. Kusada, H. Kitagawa, *Acc. Chem. Res.* **2015**, *48*, 1551 – 1559.
[2] S. Gonzalez, C. Sousa, F. Illas, *Int. J. Mod. Phys. B* **2010**, *24*, 5128 – 5138.
[3] a) J. S. Foord, P. D. Jones, *Surf. Sci.* **1985**, *152 – 153*, *Part 1*, 487 – 495; b) C. T. Campbell, *Annu. Rev. Phys. Chem.* **1990**, *41*, 775 – 837; c) S. Gonzalez, C. Sousa, F. Illas, *J. Catal.* **2006**, *239*, 431 – 440.
[4] a) S. Kacimi, J. Barbier, R. Taha, D. Duprez, *Catal. Lett.* **1993**, *22*, 343 – 350; b) P. Reyes, G. Pecchi, J. L. G. Fierro, *Langmuir* **2001**, *17*, 522 – 527; c) B. Coq, R. Dutartre, F. Figueras, A. Rouco, *J. Phys. Chem.* **1989**, *93*, 4904 – 4908; d) S.-C. Chou, C.-T. Yeh, T.-H. Chang, *J. Phys. Chem. B* **1997**, *101*, 5828 – 5833; e) G. Meitzner, *J. Chem. Phys.* **1983**, *78*, 882; f) M. Fernández-García, A. Martínez-Arias, I. Rodríguez-Ramos, P. Ferreira-Aparicio, A. Guerrero-Ruiz, *Langmuir* **1999**, *15*, 5295 – 5302.
[5] D. J. Chakrabarti, D. E. Laughlin, *Bull. of Alloy Phase Diagr.* **1982**, *2*, 460 – 462.
[6] S. Priya, K. T. Jacob, *J. Phase Equilib.* **2000**, *21*, 342 – 349.
[7] A. Fritz, V. Pitchon, *Appl. Catal. B* **1997**, *13*, 1 – 25.
[8] S. Roy, M. S. Hegde, G. Madras, *Appl. Energy* **2009**, *86*, 2283 – 2297.
[9] F. Garin, *Appl. Catal. A* **2001**, *222*, 183 – 219.
[10] K. I. Choi, M. A. Vannice, *J. Catal.* **1991**, *131*, 22 – 35.
[11] F. M. T. Mendes, M. Schmal, *Appl. Catal. A* **1997**, *163*, 153 – 164.
[12] a) R. Hoffmann, *Rev. Mod. Phys.* **1988**, *60*, 601 – 628; b) M. H. Cohen, M. V. Ganduglia-Pirovano, J. Kudrnovský, *Phys. Rev. Lett.* **1994**, *72*, 3222 – 3225; c) S. Gonzalez, F. Illas, *Surf. Sci.* **2005**, *598*, 144 – 155.
[13] a) B. Hammer, J. K. Nørskov in *Theoretical surface science and catalysis—calculations and concepts, Vol. 45* Academic Press, **2000**, pp. 71 – 129; b) B. Hammer, Y. Morikawa, J. K. Nørskov, *Phys. Rev. Lett.* **1996**, *76*, 2141 – 2144; c) F. Illas, N. López, J. M. Ricart, A. Clotet, J. C. Conesa, M. Fernández-García, *J. Phys. Chem. B* **1998**, *102*, 8017 – 8023; d) J. K. Nørskov, T. Bligaard, J. Rossmeisl, C. H. Christensen, *Nat. Chem.* **2009**, *1*, 37 – 46; e) B. Hammer, M. Scheffler, *Phys. Rev. Lett.* **1995**, *74*, 3487 – 3490.
[14] L. Huey-Lin, P. Duwez, *J. Less-Common Met.* **1964**, *6*, 248 – 249.
[15] M. J. Sharif, S. Yamazoe, T. Tsukuda, *Top. Catal.* **2014**, *57*, 1049 – 1053.

Received: September 11, 2016
Accepted Article published: October 27, 2016
Published online on November 23, 2016

